

Interpretation of the Time Constants Measured by Kinetic Techniques in Nanostructured Semiconductor Electrodes and Dye-Sensitized Solar Cells

Juan Bisquert*[†] and Vyacheslav S. Vikhrenko[‡]

Departament de Ciències Experimentals, Universitat Jaume I, 12080 Castelló, Spain, and
Belarussian State Technological University, Minsk, 220050 Belarus

Received: May 20, 2003; In Final Form: November 18, 2003

The processes of charge separation, transport, and recombination in dye-sensitized nanocrystalline TiO₂ solar cells are characterized by certain time constants. These are measured by small perturbation kinetic techniques, such as intensity modulated photocurrent spectroscopy (IMPS), intensity modulated photovoltage spectroscopy (IMVS), and electrochemical impedance spectroscopy (EIS). The electron diffusion coefficient, D_n , and electron lifetime, τ_n , obtained by these techniques are usually found to depend on steady-state Fermi level or, alternatively, on the carrier concentration. We investigate the physical origin of such dependence, using a general approach that consists on reducing the general multiple trapping kinetic-transport formalism, to a simpler diffusion formalism, which is valid in quasi-static conditions. We describe in detail a simple kinetic model for diffusion, trapping, and interfacial charge transfer of electrons, and we demonstrate the compensation of trap-dependent factors when forming steady-state quantities such as the diffusion length, L_n , or the electron conductivity, σ_n .

1. Introduction

Spatially heterogeneous mixtures of nanometer-scale constituents form new classes of solar cells. These solar cells, consisting on a combination of semiconductor nanoparticles, redox electrolytes, conducting polymers and photoactive organic molecules, are quite appealing due to easy processability of the materials in a large scale, showing promise for cheap and versatile photovoltaic devices.¹ The dye-sensitized solar cell (DSSC) is a heterogeneous solar cell where the carriers transferring the chemical energy created in an excited dye are electrons in nanocrystalline TiO₂ and redox species in a liquid electrolyte. Besides being highly efficient for light to electrical energy conversion, the DSSC is a good model system for the heterogeneous photovoltaic converters because the different phases in it are continuously connected and physically separated.

In general, the heterogeneous configuration is widely investigated because it has the advantage of providing a huge internal area where charge separation can be realized following excitation of the light absorber. It is also essential for the conversion efficiency to maintain the separated carriers in their respective nanoscaled independent channels until they are collected at the contacts. Therefore, the determination of quantities such as the diffusion coefficient and the lifetime of the different carriers becomes a central issue in the investigation of these devices. These time constants are obtained by small perturbation kinetic measurements that do not modify the steady state over which they are measured. Examples of the techniques are intensity modulated photocurrent spectroscopy (IMPS), intensity modulated photovoltage spectroscopy (IMVS), electrochemical impedance spectroscopy (EIS), and small amplitude time transients.

The results of these techniques in nanostructured semiconductors and DSSCs indicate the dependence of the electron

diffusion coefficient on the electrochemical potential of electrons, $\bar{\mu}_n$ (also denoted quasi-Fermi level, E_{Fn}).^{2–9} For DSSCs, a large variation of the electron lifetime with increasing light intensity has been reported as well.^{5,10,11} From these observations, it is often inferred that trapping mechanisms mediate transport and recombination in nanostructured semiconductors permeated with a conductive phase.^{2,5,6,12–14} A major research effort has been aimed toward measuring the “effective” variable diffusion coefficient, D_n , and the “effective” variable lifetime, τ_n , observed in DSSCs in different conditions. In this paper, we aim at a better physical understanding of these effective parameters.

An interesting observation on the effective D_n and τ_n has been indicated by Peter and co-workers. They found that in some cases the product of these quantities compensates to a large extent, forming a nearly constant electron diffusion length, L_n .^{5,15} On another hand, recent measurements¹⁶ of the electronic conductivity, σ_n , of nanostructured TiO₂ in aqueous electrolyte show an increase of nearly 60 mV/decade over a wide range of Fermi level positions with respect to the conduction band potential. This dependence can be explained by an expression of the type

$$\sigma_n = \frac{e^2}{k_B T} n_c D_0 \quad (1)$$

where n_c is the density of free electrons in the conduction band, D_0 is the constant diffusion coefficient for free electrons, e is the positive elementary charge and $k_B T$ is the thermal energy. Thus, it appears that quantities that can be measured at steady-state, such as L_n and σ_n , do not contain the information on trapping and detrapping effects that is obtained when D_n is measured directly by kinetic techniques.

From these and other results, it appears relevant to clarify the interpretation of photophysical quantities measured in nanostructured semiconductors and DSSCs, considering both

* To whom correspondence should be addressed. E-mail: bisquert@uji.es.

[†] Universitat Jaume I.

[‡] Belarussian State Technological University.

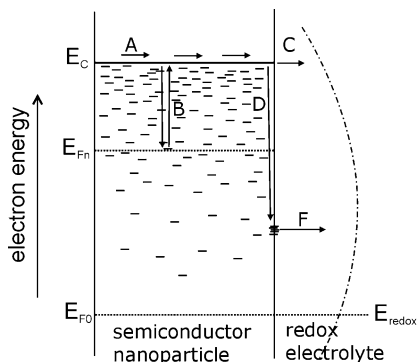


Figure 1. Schematics of the steps involved in transport of the photoinjected electron and the recombination with the oxidized species in the electrolyte in a dye-sensitized solar cell. (E_{F0}) shows the position of the Fermi level in the dark, equilibrated with the redox potential (E_{redox}) of the acceptor species in solution. (E_{Fn}) is the (quasi)Fermi level of electrons under illumination and E_c is the conduction band energy. The following steps are indicated: (A) Electron transport through extended states; (B) electron capture and thermal release at an exponential distribution of band gap localized states; (C) electron transfer through conduction band to the fluctuating energy levels of oxidized species in solution indicated in the right; (D) capture by and (F) charge transfer through surface states.

the time constants obtained from kinetic measurements and the steady-state quantities such as the electron diffusion length, the electron conductivity, and the incident photon-to-current conversion efficiency (IPCE). Indeed, both classes of parameters indicate a different kind of information. The former refer to the time for recovery of equilibrium, either by transport or recombination, i.e., they correspond to a switching time, whereas the latter refer to stationary operation and determine the photovoltaic efficiency of the device.

It is important, therefore, to examine the relationship of time constants D_n and τ_n , obtained from macroscopic evolution of carrier densities, to the microscopic assumptions on electronic transitions and distribution of states, to see how these constants, describing in principle different phenomena in the solar cell, relate to each other and how they behave when they are combined to form other important quantities such as the IPCE. To analyze these questions, we outline a relatively simple kinetic model for diffusion, trapping and interfacial charge transfer of electron carriers in a nanostructured semiconductor permeated with a redox electrolyte. We will use the multiple trapping (MT) model for transport and charge transfer illustrated in Figure 1. This model is adapted to nanostructured semiconductors from a wide experience on disordered semiconductors. The MT transport, is summarized by Shmidlin¹⁷ and Tiedje and Rose,¹⁸ and was applied first by Vanmaeckelbergh² for nanoporous semiconductors, and extended by many workers in the DSSC area.^{2,5,6,9,12} The key feature of the MT framework is the restriction that only free electrons contribute to the diffusion current.¹⁷ Diffusion by direct hopping between localized states is also possible in materials with a wide distribution of traps, but this mechanism will not be considered in this paper. For trapping and recombination, the ideas formulated by Rose¹⁹ can be adapted to DSSC as indicated in ref 11. Here we combine both aspects, MT transport and recombination, in a single model that may be considered a working model that gives an overall view of the more relevant phenomena in the DSSC and shows clearly the interconnection between measured quantities. The meaning of the Fermi-level dependence of D_n and τ_n will become transparent in terms of trapping factors and we will show the compensation of these trapping factors when we form the steady-state quantities L_n and IPCE.

2. Chemical Diffusion Coefficient

2.1. Kinetic-Transport Formalism. We state the kinetic-transport equations in the MT model for a single kind of trap, consisting on the equations of conservation for free and trapped electrons and Fick's law for the free electrons:¹⁷

$$\frac{\partial n_c}{\partial t} = -\frac{\partial J}{\partial x} - \beta n_c [1 - f_L] + \epsilon N_L f_L \quad (2)$$

$$\frac{\partial f_L}{\partial t} = \beta \frac{n_c}{N_L} [1 - f_L] - \epsilon f_L \quad (3)$$

$$J = -D_0 \frac{\partial n_c}{\partial x} \quad (4)$$

Here N_L is the total density of localized sites (per unit volume), f_L is the fractional occupancy ($n_L = N_L f_L$), and J is the diffusive flux of conduction band electrons. The rate constant for electron capture is determined by the thermal velocity of free electrons, v , the electron capture cross section of the trap, s_n , and the density of traps, N_L

$$\beta = N_L v s_n \quad (5)$$

The rate constant for electron thermal release from the trap to the conduction band is related to β by Shockley–Read–Hall statistics²⁰

$$\epsilon = \frac{N_c}{N_L} \beta \exp[-(E_c - E_L)/k_B T] \quad (6)$$

Here, E_c is the lower band edge energy, E_L is the energy of the localized state in the band gap, and N_c is the effective density of conduction band states. Equations 2–4 can be readily extended to a distribution of localized levels. We have omitted in these equations the rate of interfacial charge transfer (recombination) which will be considered in section 3.

From eq 3 in steady state, $\partial f_L / \partial t = 0$, it follows that the electrons in the free and localized states maintain an equilibrium with a common value of the Fermi level, $\bar{\mu}_n$. The occupancies in the two kinds of states are given explicitly by

$$n_c = N_c e^{(\bar{\mu}_n - E_c)/k_B T} \quad (7)$$

$$f_L = \frac{1}{1 + e^{(E_L - \bar{\mu}_n)/k_B T}} \quad (8)$$

Note that, in eqs 7 and 8, the Fermi level $\bar{\mu}_n$ can be maintained at a different value than the redox potential in solution, E_{redox} (assuming that the exchange of electrons at the oxide/solution interface is slow). This is a *constrained* equilibrium²¹ of the system formed by the electrons in extended and localized states in the nanoporous semiconductor in contact with redox electrolyte. If the constraint (bias potential or illumination) is removed, then the system equilibrates all of the electrons at the same electrochemical potential, and in this case, $\bar{\mu}_n$ has the unique value E_{redox} .

We now define the conditions that enable the reduction of the MT framework of eqs 2–4 to the conventional diffusion equations, consisting in the ordinary conservation equation and Fick's law.

2.2. Quasiequilibrium Condition. In general the quasi-static condition applies in thermodynamic processes that are sufficiently slow for the change to consist in a succession of

equilibrium states. In our case, we are considering a system composed by two classes of electronic states, initially at (constrained) equilibrium indicated by the common value of the temperature and the electrochemical potential in eqs 7 and 8.

When equilibrium at $\bar{\mu}_n$ is perturbed by some external cause (for example, injecting Δn_c electrons to the conduction band), the subsequent variations ($\partial n_c/\partial t$) and ($\partial n_L/\partial t$) are ruled by the instantaneous occupancies and transition rates described in eqs 2–4. We define a particular kind of evolution as that which obeys the quasistatic condition

$$\frac{\partial n_L}{\partial t} = \frac{\partial n_L}{\partial n_c} \frac{\partial n_c}{\partial t} \quad (9)$$

so that free and trapped electrons maintain a common equilibrium even when the system is displaced away from equilibrium. In practice, this implies that trap relaxation is much faster than the frequency/times of interest in the measured phenomena, for instance, faster than the transit time through the film while measuring diffusion coefficient. Equation 9 may be written alternatively in terms of kinetic factors for trapping and detrapping, $\partial n_L/\partial n_c = \beta/\epsilon$. However, normally the principle of detailed balance (that states that for a system in thermal equilibrium, the rates of a process and of its inverse are equal and balance in detail) is taken as a representation of microscopic reversibility.²² Given the rate constant β , detailed balance gives ϵ in eq 6 through the equilibrium occupancies.²⁰ So the factor $\partial n_L/\partial n_c$ between equilibrium occupancies in eq 9 appears more fundamental in order to assert that the proportion of the rates of change of populations of localized and free electrons, $(\partial n_L/\partial t)/(\partial n_c/\partial t)$, maintains those populations at the common equilibrium values.

We remark that the factor $(\partial n_L/\partial n_c)$ is not the proportion of number of carriers, but rather the relation of variations induced during the small perturbation that leaves invariant the steady state. Incidentally, it is found that $\partial n_L/\partial n_c \propto n_L/n_c$ in some cases (as in exponential distribution of traps), but this is not generally true.

It is generally possible to establish the time scale of the trapping-detrapping phenomena, and the time constant of the process under consideration must be considerably longer to guarantee the possibility of using the quasi-equilibrium relation between n_c and f_L . In the limit of long waves the relaxation time for trapping-detrapping is determined by the expression $\tau_i^{-1} = \beta(1 - f_L + n_c/N_L) + \epsilon$. Long waves mean that $k^2 \ll (D_0\tau)^{-1}$, where k is the wave vector determining the characteristic spatial nonhomogeneities. n_c and f_L correspond to some quasiequilibrium value of the chemical potential. In frequency methods, the characteristic patterns of relaxation functions show the onset of traps relaxation at $\omega \approx \tau_i^{-1}$, see, for example, refs 23 and 24. There are conditions in which eq 9 is not satisfied in the frequency window of the measurement, for instance if the transit time is $\ll \tau_i$; or else, if charge injection to the electrolyte is rather fast.

2.3. Reduction of Multiple Trapping to Ordinary Diffusion. Hereafter, we assume, unless otherwise stated, that the measurement operates in quasistatic conditions. From eqs 2, 3, and 9, it follows that

$$\left(1 + \frac{\partial n_L}{\partial n_c}\right) \frac{\partial n_c}{\partial t} = -\frac{\partial J}{\partial x} \quad (10)$$

Equation 10 suggests to form a new particle flux, \hat{J} , as

$$\hat{J} = -D_n \frac{\partial n_c}{\partial x} \quad (11)$$

where D_n is defined as

$$D_n = \frac{1}{1 + \frac{\partial n_L}{\partial n_c}} D_0 \quad (12)$$

and then, provided that D_n is approximately independent of position (homogeneous Fermi level), eq 2 can be expressed as

$$\frac{\partial n_c}{\partial t} = -\frac{\partial \hat{J}}{\partial x} \quad (13)$$

The new coefficient D_n obtained in eq 12 will be interpreted more generally in another paper²⁵ as the *chemical diffusion coefficient* of electrons.

Clearly, the reduction of MT to Fickian diffusion of free carriers is achieved in eqs 11–13. The simplification involves the removal of some internal degrees of freedom in the system (the occupancy of localized states) that are not explicitly resolved in the quasistatic measurement but contribute to the chemical diffusion coefficient D_n , which henceforth becomes a function of the concentration, $D_n(n_c)$, or Fermi level, $D_n(\bar{\mu}_n)$. Therefore, the experimental results of small perturbation quasistatic measurements consist on an ordinary diffusion process that takes place with the chemical diffusion coefficient, D_n . In other words, the transport-kinetic equations that describe the measured transients or frequency spectra can be considerably simplified by checking that quasiequilibrium of trapping is obeyed. In practice, this type of interpretation has been often adopted, as pointed out in the Introduction, and explained, for instance, in Appendix C of ref 26. Our analysis shows a quite general justification for this approach to the analysis of the data.

The general significance of the result in eq 12 is confirmed in particular cases found in the literature, for instance from the complete solution of the single trap model in EIS²³ and also in IMPS.²⁷ In these papers, eq 12 is obtained in the low-frequency limit of the solution of eqs 2–4 for a small perturbation in the frequency domain.

The effect of trapping in the chemical diffusion coefficient is important only insofar as $\partial n_L/\partial n_c \gg 1$, as discussed further below. Therefore, normally it is justified to reduce eq 12 to the expression

$$D_n = \left(\frac{\partial n_c}{\partial n_L}\right) D_0 \quad (14)$$

It is worth to emphasize that in general $D_n(n_c)$ and $\partial/\partial x$ do not commute, so that in conditions of nonhomogeneous steady-state Fermi level (as in IMPS) eq 13 is not valid. The correct quasi-equilibrium transport equation can be formulated using eqs 4 and 10, which give

$$\frac{\partial n_c}{\partial t} - D_0 \left(\frac{\partial n_c}{\partial n_L}\right) \frac{\partial^2 n_c}{\partial x^2} = 0 \quad (15)$$

2.4. Chemical Diffusion Coefficient in Traps Distributions.

In the quasistatic approximation the factor $(\partial n_L/\partial n_c)^{-1}$ can be calculated for any distribution of localized levels, with abundance $g(E)$ (the density of localized states, DOLS, at the energy E in the band gap) and occupancies $f_L(E - \bar{\mu}_n)$, using the equilibrium distribution of free and trapped carriers indicated

in eqs 7 and 8. In the approximation of the zero temperature limit of the Fermi function, i.e., a step function at $E = \bar{\mu}_n$ separating occupied from unoccupied states, a change of Fermi level implies a change of localized charge corresponding to the DOLS

$$\frac{\partial n_L}{\partial \bar{\mu}_n} = g(\bar{\mu}_n) \quad (16)$$

On another hand, for free electrons, the Boltzmann statistics of eq 7 gives

$$\frac{\partial n_c}{\partial \bar{\mu}_n} = \frac{n_c}{k_B T} \quad (17)$$

therefore

$$\frac{\partial n_L}{\partial n_c} = \frac{k_B T}{n_c} g(\bar{\mu}_n) \quad (18)$$

From eqs 14 and 18 a general expression is found of the chemical diffusion coefficient:

$$D_n = \frac{n_c}{k_B T} g(\bar{\mu}_n)^{-1} D_0 \quad (19)$$

We illustrate this general expression with the derivation of two cases obtained in previous works.^{5,8,9,12}

For the box distribution of width ϵ_L

$$g(E) = N_L / \epsilon_L \quad (20)$$

one gets

$$\frac{\partial n_L}{\partial n_c} = \frac{N_L k_B T}{n_c \epsilon_L} \quad (21)$$

hence

$$D_n = \frac{n_c \epsilon_L}{N_L k_B T} D_0 \quad (22)$$

which explains the phenomenological generalized diffusion equations (with $D_n \propto n_c$) used in ref 3 for analyzing transient photocurrents.

For the exponential distribution with tailing parameter T_0 (with $\alpha = T/T_0$)

$$g(E) = \frac{N_L}{k_B T_0} \exp[(E - E_c)/k_B T_0] \quad (23)$$

we obtain from eqs 7 and 18

$$\frac{\partial n_L}{\partial n_c} = \alpha \frac{N_L}{N_c} n_c^{\alpha-1} \quad (24)$$

and it follows that

$$D_n = \frac{N_c^\alpha}{\alpha N_L} n_c^{1-\alpha} D_0 \quad (25)$$

The result $D_n \propto I_0^{1-\alpha}$, derived in equation A.11 of ref 26 for the effective diffusion coefficient dependence on light intensity, I_0 , is similar to eq 25, assuming that $n_c \propto I_0$. Experimental observations do show the power-law dependence of the mea-

sured, chemical diffusion coefficient on concentration or light intensity,^{5,28} so that MT with the exponential tail of band gap states indicated in eq 23 seems a plausible model for the DSSC.

Taking into account that

$$n_L = \int_{E_c}^{E_c} g(E) f_L(E - \bar{\mu}_n) dE = N_L \exp[(\bar{\mu}_n - E_c)/k_B T_0] \quad (26)$$

and using eq 7, it follows that

$$n_L = \frac{N_L}{N_c^\alpha} n_c^\alpha \quad (27)$$

In multiple trapping conditions $n_L \gg n_c$, i.e., the total charge $n_{\text{tot}} \approx n_L$; therefore, eq 25 can be written in terms of total electron density in the following way

$$D_n = \frac{N_c}{\alpha N_L^{1/\alpha}} n_{\text{tot}}^{(1-\alpha)/\alpha} D_0 \quad (28)$$

It should be remarked that a continuous trap distribution usually causes specific patterns of anomalous diffusion. An analysis of frequency features for multiple trapping diffusion in the presence of an exponential DOLS is presented in ref 29. The time domain equations for fractional time diffusion in MT are discussed in ref 30.

3. Electron Lifetime (Response Time)

The analysis of the time constant for recombination in nanostructured semiconductors requires to consider two essential factors represented in the scheme of Figure 1.

First, the bulk of a nanoparticle may contain a large density of traps, e.g., with the exponential form of eq 23, where trapping and detrapping phenomena take place, identical to those analyzed before in relation with diffusion (process B).

On another hand, recombination is an interfacial charge-transfer event and occurs in the surface only. Charge transfer may involve a variety of interfacial mechanisms (conduction band and surface states, as indicated in Figure 1).³¹ Let us assume for the moment that recombination occurs preferentially through the conduction band (process C), at a rate

$$U_0 = - \frac{n_c}{\tau_{n0}} \quad (29)$$

so that τ_{n0} is the constant free carrier lifetime; that is, the lifetime with respect to injection to the electrolyte, in the absence of trapping.

The measurement of the electron lifetime consists of determining the time for the system to recover equilibrium under a small perturbation of the steady state, by removal of the excess carriers by recombination.¹¹ In DSSC, the lifetime can be determined by monitoring directly the variation of the position of the Fermi level with time (open-circuit photovoltage decay technique, OCVD).¹¹ To describe this evolution, one can solve the kinetic eqs 2–4, where eq 29 is an additional term in eq 2. However, this is not necessary provided that certain conditions are satisfied. The effect of trapping and detrapping in the bulk is simplified by the quasi-equilibrium condition of eq 9, provided that the rate constants for trapping and detrapping are much faster than τ_{n0} . Therefore, the displacement of the Fermi level involves the recombination by interfacial charge transfer of both the trapped and free charge, and the observed time constant is considerably longer than τ_{n0} .¹⁹ Furthermore, the process of

conduction band transport (A) is assumed to be also fast so that no relevant inhomogeneities of charge exist (this point is further discussed in the Appendix). Then the time constant for the decay takes the form

$$\tau_n = \left(1 + \frac{\partial n_l}{\partial n_c}\right) \tau_{n0} \quad (30)$$

as shown in detail in a recent paper.¹¹ Equation 30 was formulated for amorphous semiconductors by Rose,¹⁹ and the observed recombination time, τ_n , is denoted the response time. In the case $\partial n_l/\partial n_c \gg 1$, in which trapping and detrapping governs the response time, eq 30 can be simplified

$$\tau_n = \left(\frac{\partial n_l}{\partial n_c}\right) \tau_{n0} \quad (31)$$

Equation 31 implies a Fermi-level dependence of τ_n as we have seen above for D_n . Using the exponential distribution of eq 23 in eq 31, we obtain with eq 24 the power law form on free electron concentration (exponential dependence on illumination intensity) that is usually found in measurements¹¹

$$\tau_n = \frac{\alpha N_c}{N_c^\alpha} n_c^{\alpha-1} \tau_{n0} \quad (32)$$

Besides injection from the conduction band, another important recombination channel is a two-step process involving trapping at band-gap surface states (D) and subsequent isoenergetic transfer to electrolyte levels (F). In addition, there may exist a distribution of surface states that participate in charge transfer.¹⁰ The different possibilities have been analyzed theoretically in ref 31, but experimentally, the details about the relevant levels for charge transfer have not yet been clarified, and the subject lies outside the scope of the present work. However, it is important to realize that the result of eq 31 is valid generally in the quasiequilibrium conditions stated above.¹¹ Indeed, the previous argumentation is the same when the quantity τ_{n0} of eq 31 involves a combination of interfacial mechanisms. In this case, however, τ_{n0} may acquire its own dependence on the steady state, as discussed in ref 11. In this paper, it was shown that eq 31 describes correctly the major features of the response time in DSSC, but more work is necessary in order to establish the details of τ_n dependence on Fermi level.

The analysis of transient decays in ref 32 in terms of microscopic models for electrons transitions provides more detailed insight into the temporal evolution of recombination mechanisms. Nelson et al.³² pointed out that recombination in the multiple trapping regime is governed by carriers redistribution in the energy levels, and ref 33 confirmed this idea, which supports our simpler, quasiequilibrium approach. However, these papers did not calculate the steady-state time constants considered here.

4. Electron Diffusion Length

We now turn our attention to the measurements that are realized in steady-state conditions, for instance by measuring the photocurrent in the solar cell at a constant incident illumination. In those cases, imposing $\partial n_c/\partial t = 0$ and $\partial n_l/\partial t = 0$, eqs 2–4 reduce to

$$D_0 \frac{\partial^2 n_c}{\partial x^2} - \frac{n_c}{\tau_{n0}} + G = 0 \quad (33)$$

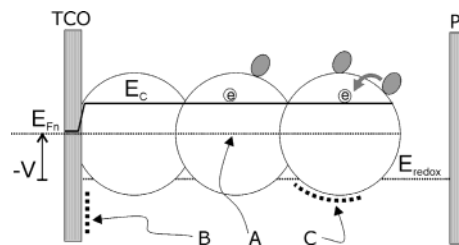


Figure 2. Schematics of the capacitive contributions in a dye-sensitized solar cell: (A) Chemical capacitance due to increasing chemical potential (concentration) of electrons in the TiO₂ phase, obtained when the electrode potential, V , displaces the electron Fermi level, E_{Fn} , with respect to the lower edge of the conduction band, E_c , in the semiconductor nanoparticles. (B) Electrostatic capacitance of the Helmholtz layer (and semiconductor bandbending) at the interface between the exposed surface of the transparent conducting oxide substrate and the electrolyte. (C) Electrostatic capacitance at Helmholtz layer at the oxide/electrolyte interface.

The remaining transport equation is equivalent to the standard diffusion model for DSSC³⁴ and contains no information on trapping. This is because in the steady state the traps simply adjust their occupancy to the Fermi level. Accordingly the diffusion length is given by a constant, $L_n = \sqrt{(D_0 \tau_{n0})}$. The IPCE, which depends only on L_n and geometrical factors,³⁴ is also constant. Both L_n and IPCE can be measured from the steady-state photocurrent.

On the other hand, determinations of the diffusion coefficient and lifetime by kinetic measurements provide D_n and τ_n , as discussed in the previous sections. However, from eqs 12 and 31, we realize that the factors $(\partial n_l/\partial n_c)$ in D_n and τ_n compensate when forming the diffusion length from measured quantities. The result is a constant consistent with eq 33

$$L_n = \sqrt{D_n \tau_n} = \sqrt{D_0 \tau_{n0}} \quad (34)$$

The meaning of the compensation is clear when we note that the origin of the factor $(\partial n_l/\partial n_c)$ lies in carrier equilibration in the energy space (process B in Figure 1), both for chemical diffusion coefficient in MT (D_n), and for response time (τ_n). Peter and co-workers^{5,15} and also Nakade et al.²⁸ have reported for DSSCs the compensating behavior indicated in eq 34.

5. Chemical Capacitance

In the previous sections, the DOLS of electrons was seen to exert a considerable influence over the measured time constants. Fortunately, the DOLS can be determined quite directly in nanostructured semiconductors, by measurements of capacitance. It is convenient to emphasize the direct relationship between the measured capacitance and thermodynamic function (chemical potential) of electrons, otherwise one may lose valuable information by attempting to determine the capacitance in terms of conventional ideas of dielectric constant and space-charge regions. Therefore, we try to clarify the point in the following discussion.

5.1. Electrostatic and Chemical Capacitors. The capacitance of nanoporous semiconductor films can be determined in several ways: EIS,^{35,36} cyclic voltammetry,³⁷ or integrating the current at differential voltage steps.³⁸ There are several physical effects contributing to the measured capacitance, as indicated in Figure 2. The process (B) indicates polarization at the interface between the transparent conducting substrate (TCS) and the electrolyte, and (C) indicates the Helmholtz layer at the oxide/electrolyte interface. The former effect is important when the electron density is low in the semiconductor³⁹ and

the latter when the density is very high and the semiconductor enters the state of band unpinning. Both these contributions can be thought of as ordinary electrostatic capacitors, where the charges in two highly conducting plates sustain an electrical field in between.

In the intermediate range of Fermi level variation, a different kind of capacitive effect is found (A). The semiconductor bands are pinned, and the charge accumulation is related to the displacement of the Fermi level position with respect to the conduction band edge, i.e., to a variation of chemical potential of electrons, $\Delta\bar{\mu}_n = \Delta\mu_n$. Hence, the increment of charge (electronic and ionic) occurs in the volume of the nanostructured electrode with no concomitant electrical field variation in the volume, because the electrical field is shielded near the TCS.⁴⁰ Therefore, (free) energy storage in the capacitor is by chemical, not electrostatic, energy. As a consequence, it is a chemical capacitor, and not an electrostatic capacitor.

To appreciate the physical basis for this new concept, we remind that the impedance function can be defined generally for any thermodynamic system, and characterizes the linear response of the system to an applied force.⁴¹ Indeed, the fluctuation–dissipation theorem⁴¹ shows that the admittance is related directly to the equilibrium fluctuations of the system, and although the conductivity characterizes the irreversible response of the system, a lossless element that indicates the reversible response constitutes a capacitance.⁴² In particular, for a volume element that stores chemical energy due to a thermodynamic displacement, the chemical capacitance per unit volume is defined as⁴³

$$C = e^2 \frac{\partial N_i}{\partial \mu_i} \quad (35)$$

So the chemical capacitance reflects the capability of a system to accept or release additional carriers with density N_i due to a change in their chemical potential, μ_i .⁴³

The general physical meaning of eq 35 has been explained recently using another route.⁴⁴ In mesoscopic capacitors,⁴⁴ the electrical field related to the electrochemical potential difference between the leads is partially shielded and it cannot propagate toward the surface of the plates of the capacitor, which causes a displacement of the Fermi level with respect to the conduction band. Büttiker et al.⁴⁴ have shown that this effect introduces a factor proportional to $dn/d\mu_n$ in the electrochemical capacitance, in agreement with eq 35.

5.2. Chemical Capacitance in Nanostructured Semiconductors. The chemical capacitance (A in Figure 2) is a major feature in TiO₂ nanostructured electrodes. For instance, in measurements of these electrodes in aqueous solution, this effect causes an exponential increase of the capacitance by 3 orders of magnitude in an interval of potentials of 0.8 V.³⁷ Similar results are obtained in DSSC.³⁵ Besides, the chemical capacitance is a concept of crucial significance for solar cell applications, because it describes properly the splitting of Fermi levels caused by excitation of carriers in the light absorber material.⁴⁵

Considering the variation of the electron density upon a change of the local chemical potential in a DSSC, we obtain for the total chemical capacitance

$$C_{\text{ch}}^{(\text{tot})} = e^2 \frac{\partial(n_c + n_L)}{\partial \mu_n} \quad (36)$$

One may distinguish the two components in eq 36.⁴⁶ The first is related to the free conduction band electrons. Using eq 17,

we find

$$C_{\text{ch}}^{(\text{cb})} = e^2 \frac{\partial n_c}{\partial \mu_n} = e^2 \frac{n_c}{k_B T} \quad (37)$$

The second component of eq 36 is related to localized states in the band gap. From eq 16, it is seen readily that this component is just proportional to the DOLS at the Fermi level

$$C_{\text{ch}}^{(\text{trap})} = e^2 \frac{\partial n_L}{\partial \mu_n} = e^2 g(\bar{\mu}_n) \quad (38)$$

In the case of the exponential distribution given in eq 23, eq 38 provides the form

$$C_{\text{ch}}^{(\text{trap})} = e^2 \frac{\alpha N_L}{k_B T} e^{(\bar{\mu}_n - E_c)/k_B T_0} \quad (39)$$

We may also express eq 39 in terms of the free electron density, in which case we obtain

$$C_{\text{ch}}^{(\text{trap})} = e^2 \frac{\alpha N_L}{k_B T N_c} n_c^\alpha \quad (40)$$

The two chemical capacitors in eq 36 are connected in parallel. If it is $C_{\text{ch}}^{(\text{trap})} \gg C_{\text{ch}}^{(\text{cb})}$, as required in the trapping models, resolving $C_{\text{ch}}^{(\text{cb})}$ is not possible by simply measuring the *low frequency* capacitance, which is $C_{\text{ch}}^{(\text{tot})} = C_{\text{ch}}^{(\text{trap})} + C_{\text{ch}}^{(\text{cb})} \approx C_{\text{ch}}^{(\text{trap})}$.⁴⁷ Note that both eq 37 and 39 show an exponential dependence with the bias, although with different slopes. The ideal statistics of eq 37 give a slope $(d \log C/dV) = -e/(2.30k_B T)$, i.e., 60 mV/decade at room temperature. This is not normally found in nanostructured TiO₂. The exponential capacitance is observed with a much less steep rise, of about 300 mV/decade. This has been interpreted in terms of eq 39, i.e., the manifestation of the exponential distribution of band gap states which gives $(d \log C/dV) = -e/(2.30k_B T_0)$,^{35,37} with $T_0 \approx 1400$ K. For instance, measurements of capacitance of nanostructured TiO₂ electrodes in aqueous solution at pH 3 yield a value of $\alpha = 0.25$ and a total trap density of $N_L \approx 10^{19}$ cm⁻³.³⁷ The exponential DOLS and mentioned $(d \log C/dV)$ values are also supported by the results of a stepping charge-extraction method.⁴⁸

It must be remarked, however, that the exponential distribution that describes well different pieces of experimental data (such as the chemical diffusion coefficient and lifetime) is so far a phenomenological formula the origin of which is not well understood. So we choose to use in Figure 1 the simplest approach to describe this feature, which is a stationary distribution of electron sites related to intrinsic disorder, usually found in amorphous semiconductors. However, in doped crystalline semiconductors, the spread of conduction band states is caused by local distortion of energies near the dopant atoms. In crystalline nanoparticles surrounded by electrolyte, interaction effects between the electrons and ionic species that modify the electrons energy levels cannot be discarded to account partially for the tailing distribution.

As mentioned before, surface charging changes the potential difference in the Helmholtz layer, producing an upward shift of the semiconductor energy levels, $V_H = \Delta\phi_H$. The combined effect of electron accumulation and partial band unpinning implies that the Helmholtz capacitance, C_H , is connected in series³⁷ to the chemical capacitance, C_{ch} , so that the position of the bands will remain pinned insofar as $C_{\text{ch}} \ll C_H$.

5.3. Resolution of Free Carrier Time Constants. We have commented that the chemical capacitance provides direct information on the density of states in the nanostructured semiconductor. It is important therefore to emphasize that the measurements of capacitance indicate an exponential DOLS with much higher capacitance than the conduction band component, $C_{\text{ch}}^{(\text{trap})} \gg C_{\text{ch}}^{(\text{cb})}$, i.e., $\partial n_i / \partial n_c \gg 1$, as this is a necessary requisite for the interpretation of time constants in terms of trapping models that we have exposed in the previous sections.

This point can be expressed in quantitative form, leading to interesting consequences. Indeed note that the chemical diffusion coefficient of eq 14 for MT model may be written, alternatively, in terms of the chemical capacitances of eqs 37 and 38, as¹²

$$D_n = \frac{C_{\text{ch}}^{(\text{cb})}}{C_{\text{ch}}^{(\text{cb})} + C_{\text{ch}}^{(\text{trap})}} D_0 \quad (41)$$

So MT transport occurs when $C_{\text{ch}}^{(\text{trap})} \gg C_{\text{ch}}^{(\text{cb})}$, giving the result

$$D_n = \frac{C_{\text{ch}}^{(\text{cb})}}{C_{\text{ch}}^{(\text{trap})}} D_0 \quad (42)$$

which is identical to eq 14. Also eq 25 for the exponential DOLS can be obtained from eqs 37, 40, and 42. Similar identifications can be made with the response time of eq 31, i.e.

$$\tau_n = \frac{C_{\text{ch}}^{(\text{trap})}}{C_{\text{ch}}^{(\text{cb})}} \tau_{n0} \quad (43)$$

In the previous sections, we have remarked that the time constants measured in kinetic techniques are Fermi-level dependent, $D_n(\bar{\mu}_n)$ and $\tau_n(\bar{\mu}_n)$, as indicated in eqs 42 and 43. However, this is when the trapping degrees of freedom are obscured in the quasi-equilibrium measurement, as explained in section 2. Now eqs 42 and 43 show that it is really possible to measure the free electrons diffusion coefficient and lifetime, D_0 and τ_{n0} , which are determining the diffusion length, eq 30, but for this, it is necessary to resolve separately the free and trapped charge through the correspondent chemical capacitances.

As mentioned before, the low frequency capacitance gives only $C_{\text{ch}}^{(\text{tot})} \approx C_{\text{ch}}^{(\text{trap})}$. The EIS technique, for example, permits the observation of relaxation of the charge in extended states at high frequencies (cf. Figures 1 and 4 in ref. 23), where traps do not respond anymore (i.e., breaking quasi-equilibrium at short times). In this way, $C_{\text{ch}}^{(\text{cb})}$ would be determined from high-frequency data. Note that this procedure requires resorting to the complete impedance model including the traps relaxation.^{23,47,49}

In a similar way, it should be possible to separate free and trap components of the chemical capacitance by light absorption techniques, and this is discussed in ref 46.

5.4. Relationship of Chemical Capacitance to Diffusion. Although the manifestation of traps in the chemical capacitance is a necessary condition for MT diffusion, as already remarked, it must also be pointed out that the measurements of capacitance do not give detailed information on the diffusion process itself. Chemical capacitance indicates the equilibrium distribution of electrons in the available states of the system or, more generally, the chemical potential of electrons, but not the process of transport between those states. The capacitance does not indicate whether the localized states belong to the surface or interior of nanoparticles, which is an important issue for recombination models.

Traditionally, the chemical capacitance associated to the storage of conduction band electrons, eq 37, was observed in solid-state pn junctions at a forward bias and was termed a diffusion capacitance. This denomination, adopted recently in some papers in the DSSC area^{50,51} (and also used by us sometimes), is not very fortunate because diffusion is an irreversible energy loss process, whereas the capacitance is a reversible energy storage element. It is well-known that diffusion is caused by a local difference of chemical potentials. The chemical capacitance, distributed in space, is the element that provides a chemical potential that depends on the position. So the chemical capacitance is a prerequisite for diffusion (and this is the reason the chemical capacitance is always a component of diffusion impedance,⁴³ either in DSSCs or solid-state pn junctions^{52,53}). However, the converse is not true, the capacitance of eq 37 is not diffusional in origin.⁵³

6. Electron Conductivity

Another important quantity for many applications is the electron conductivity, which can be measured in the steady state as reported elsewhere.¹⁶ In the context of the MT model, the electron transport is carried by a single kind of state, the extended states of the conduction band. Carriers trapped in localized states do not contribute to the dc conductivity until they are released again. The conductivity related to the electron diffusion process can be obtained from the generalized Einstein relation

$$\sigma_n = e^2 \frac{\partial n_c}{\partial \mu_n} D_0 \quad (44)$$

where μ_n is the chemical potential of electrons. From eq 37, we can write eq 44 as

$$\sigma_n = C_{\text{ch}}^{(\text{cb})} D_0 \quad (45)$$

and the standard expression of eq 1 is obtained with the second equality of eq 37.

Let us analyze the conditions required for determining the free carrier diffusion coefficient from the conductivity. From eq 42, we can write the conductivity also as

$$\sigma_n = C_{\text{ch}}^{(\text{trap})} D_n(\bar{\mu}_n) = e^2 g(\bar{\mu}_n) D_n(\bar{\mu}_n) \quad (46)$$

The first equality of eq 46 shows that the quotient of quantities σ_n / C_{ch} , which can be measured at low frequency, gives the chemical diffusion coefficient D_n , so again we need $C_{\text{ch}}^{(\text{cb})}$ for obtaining D_0 . From eq 1, we can obtain D_0 from σ_n if $n_c(E_c - \bar{\mu}_n)$ is known, but this also requires to resolve the free electrons component of the chemical capacitance.

7. Final Remarks and Conclusion

In this paper, we have discussed the interpretation of photoelectrochemical techniques in nanoporous semiconductor electrodes in terms of the model for electron diffusion, trapping in the bulk and recombination indicated in Figure 1. We argued that the effects of trapping appear in transient and kinetic quantities but not in steady-state quantities. Time constants such as the chemical diffusion coefficient, D_n , and electron response time, τ_n , are measured by means of small perturbation of the steady state. These time constants acquire dependencies on the steady-state Fermi level due the presence of internal degrees of freedom corresponding to trapping and detrapping of electrons that are not observed separately. In contrast, the free carrier

diffusion coefficient, D_0 , and the free carrier lifetime, τ_{n0} , cannot be measured separately using techniques at quasi-equilibrium conditions. However, the free carrier time constants can be inferred from D_n , τ_n , and total charge relaxation $C_{ch}^{(tot)}$, all of which can be measured at low frequencies, provided that additional information on *free carrier density* is available. In addition, quantities such as L_n , σ_n , and IPCE can be measured directly in the steady state. Kinetic effects of the multiple trapping disappear in L_n , σ_n , and IPCE, because in the steady state the trap occupancy remains stationary.

Illustrations of our interpretation of measured time constants with impedance²³ and optoelectrical techniques (IMPS)²⁷ have been mentioned. Another example of this is found in the model of Vanmaekelbergh et al.⁴ that considers a combination of processes in nanoporous TiO₂ electrodes in aqueous solution. It can be seen from their results of the optoelectrical transfer function (IMPS) (see eqs 15 and 20 in ref 4) that the low-frequency limit, $\Delta i_n/e\Phi(0)$, corresponding to steady-state photocurrent quantum yield, is independent of internal traps parameters. On the contrary, the IMPS frequency ω_{min} , related to the transit time as $\tau_d = 2.5/\omega_{min}$,⁴ is mainly determined by trapping factors.

Having introduced different diffusion coefficients, i.e., the chemical and free carrier diffusion coefficients, we may ask which is their relative significance. D_n provides the time for restoring equilibrium by transport when an excess of carriers is injected, whereas D_0 determines (with the carrier density) the carrier flux at the steady state. So one may be more interested in one or the other depending on the particular device and application. For instance in photocopiers the transient behavior of excess carriers generated by a flash of light, indicated by D_n , is crucial, and this led H. Scher and others to identify the anomalous transient-time dispersion.⁵⁴ In contrast, for solar cells, the main issue is the collection efficiency at steady state. According to the model illustrated in Figure 1, the compensation of the density-dependence of both chemical diffusion coefficient and response time (lifetime) is absolute, giving a strictly constant diffusion length, hence, D_0 , and the free carrier lifetime, τ_{n0} , appear to be the central physical parameters determining the solar cell operation. Nonetheless, we remark that frequency or time transient methods remain essential for the characterization of heterogeneous solar cells such as DSSC. Clearly, information on quantities such as D_n and τ_n is necessary in order to obtain a picture of the dynamic behavior of the solar cell, and to clarify the transport and recombination phenomena that are relevant for steady-state operation.

The model outlined in Figure 1, based on the contributions of many workers, provides a description of disorder in nanostructured TiO₂, through the traps distribution, and shows good agreement with the main features of the measured chemical diffusion coefficient of electrons, ranging from 10⁻⁴ to 10⁻⁸ cm²/s depending on light intensity^{8,27} and also with the electron lifetime dependence on open-circuit photovoltage.¹¹ To inquire further which is the degree of reality of this simple model, and how it should be improved, let us emphasize the main physical assumption behind the model: it is that there are many electron traps that do not act as recombination centers. For nanostructured TiO₂ the obvious realization of this feature is that there are both internal traps and surface states in the nanoparticles, as suggested in the scheme of Figure 1. Further evidence for the distinction between internal traps and surface states remains important for establishing this picture.

One way to approach this question is to change the size of particles in the electrodes, thus modifying the surface-to-volume

ratio. Recent results of Nakade et al.⁵⁵ using this method show that modification of the particles surface (by dye adsorption) enhances the chemical diffusion coefficient significantly, while maintaining the light-intensity dependence of D_n . The authors⁵⁵ remarked that these results indicate the presence of electron traps located inside the nanoparticles. Indeed, in terms of Figure 1, when traps near the surface are removed, the total density N_L decreases, and $\partial n_c/\partial n_L$ in eq 14 increases by a constant value while the dependence of D_n on E_{Fn} persists.

In relation to this question, we comment in the Appendix on the very interesting results of Kopidakis et al.⁵⁶ that were published when this paper was nearly completed.

We have emphasized in this report that the factor $(\partial n_L/\partial n_c)$ imparts a Fermi level-dependence to the time constants measured in quasistatic conditions such as $D(\bar{\mu}_n)$ and $\tau(\bar{\mu}_n)$. Considering for instance $D_n(\bar{\mu}_n)$ in eq 14, it is appreciated that the kinetic characteristics of transport appear through the conduction band diffusion coefficient, D_0 , which is a constant, whereas the variable factor $(\partial n_L/\partial n_c)$ is related to local redistribution of charge in the energy axis when the Fermi level is modified. Similar remarks can be made about $\tau(\bar{\mu}_n)$ in eq 27. So the "time constants" $D_n(\bar{\mu}_n)$ and $\tau_n(\bar{\mu}_n)$ contain different components that are either kinetic or thermodynamic in origin. It is interesting to carry out this distinction precisely, as one may be able to extract relevant consequences from models without having to solve them completely. This question is investigated specifically in a separate report for the chemical diffusion coefficient.²⁵

Acknowledgment. This work was supported by Fundació Caixa Castelló under Project P11B2002-39.

Appendix: Diffusion-Limited Recombination

The authors of ref 56 have measured the time constants of DSSCs with careful consideration to maintaining a homogeneous steady state and applying small perturbation, so the results reported are the chemical diffusion coefficient, D_n , and lifetime (response time), τ_n , that we have discussed above. We first comment the many common aspects of their explanation and ours, based on their observation of the features of time constants under modification of the thermodynamic function of electrons by lithium intercalation. Thereafter, we consider a point of contrast concerning the interpretation of the measured lifetime, τ_n .

In ref 56, lithium ions were intercalated into TiO₂ in DSSCs to substantial levels, either potentiostatically or illuminating the solar cells for a long time. This modified the shape of the exponential distribution for electrons, indicated by a large change of the tailing parameter α that is determined from $D_n(n_{tot})$ in eq 28, which is similar to eq 4c of ref 56. Furthermore, a linear model for recombination is formulated in ref 56 to obtain $\tau_n(n_{tot})$. In common with previous reports,^{5,15,28} Kopidakis et al. find the conjugate tendencies in D_n and τ_n dependence on electron concentration that leads to their compensation in L_n , as we have also discussed, and this is maintained even under variation of α . The authors also confirm that these huge changes in the distribution of electron traps have only a small effect on the collection efficiency of the solar cell, and they remark on the significance of this point, which we have discussed also. So the results of this report,⁵⁶ and the explanation suggested by its authors, are much in agreement and provide strong support for the general approach to the interpretation of time constant presented here.

We also wish to comment on a point of contrast between the interpretation of the recombination mechanism in ref 56 and

our approach presented in section 3. The other report⁵⁶ bases the interpretation of the response time τ_n on a diffusion-limited (or transport-limited) recombination process. The Fermi level-dependence of the response time is obtained in their eq 12 from the measured diffusion coefficient in the form $\tau_n \propto 1/D_n$ (our notation). This follows also from our eqs 14 and 31; however, it should be noted that our expression for τ_n in eq 31¹¹ obtains the factor $(\partial n_V/\partial n_c)$ directly from arguments of quasiequilibrium of free and trapped electron density, so that eq 31 does not contain diffusion parameters, in contrast to eq 12 of ref 56. Therefore, our model explains all the experimental results of ref 56 without assuming a diffusion-limited recombination mechanism.

This difference of interpretation raises an interesting point. The meaning of macroscopic time constants becomes a critical issue for discerning microscopic mechanisms, as the observed dependencies can be understood in different ways. So we should like to make a precision on the model of ref 56, and by the way, we clarify also one of the aspects of our model of section 3. The relationship $\tau_n \propto 1/D_n$ indicated in ref 56 could be misleading, because the measured D_n is the chemical diffusion coefficient that describes diffusion under a macroscopic gradient of concentration.²⁵ That is, D_n governs the flux that is measured in the transients of photocurrent of Figure 1a of ref 56. However, during the open-circuit photovoltage decays of Figure 1b of ref 56 for measuring τ_n , there are no such macroscopic fluxes, because the electron distribution is basically homogeneous at each time. The only option for gradients to occur seems to be from the center to the surface of individual particles. For the measured chemical diffusion coefficient of electrons on the order of $D_n = 10^{-5} \text{ cm}^2 \text{ s}^{-1}$ and particles of radius $a = 10 \text{ nm}$, the time of equilibration of concentration gradients into TiO_2 nanoparticles is $\tau_{\text{dif}} \approx a^2/D_n = 10^{-7} \text{ s}$, whereas the OCVD takes a much larger time, on the order of $\tau_n = 10^{-1} \text{ s}$. This is why the electron density can be assumed *homogeneous* during the measurement of τ_n , as argued in section 3, so that the diffusion coefficient does not appear in our eq 31. In comparison, the circumstances are very different for the lithium intercalation process that is considered by Kopidakis et al., because the chemical diffusion coefficient of lithium ions in metal oxides can be as low as $D_{\text{ch(Li)}} = 10^{-12} \text{ cm}^2 \text{ s}^{-1}$,⁵⁷ so that the time for equilibration of gradients is $\tau_{\text{dif}} \approx a^2/D_{\text{ch(Li)}} = 1 \text{ s}$, and may dominate the intercalation phenomena.⁵⁸

Indeed, the former point is clear to Kopidakis et al., as their argument does not involve any concentration gradients of electrons during OCVD but a scarcity of acceptor species that obliges the electron to effect a long random displacement over thousands of nanoparticles before it can recombine. So the relationship assumed in ref 56 for diffusion-limited recombination should be $\tau_n \propto 1/D_J$, where D_J is the jump (or tracer) diffusion coefficient that describes the random walk of electrons.²⁵ This comes to no importance for their argument, because in the case of the exponential distribution of traps the thermodynamic factor, χ_T , that relates both diffusion coefficients, $D_n = \chi_T D_J$, is a constant, $\chi_T = 1/\alpha$, as we show in another report,²⁵ so indeed the random walk of an electron, governed by D_J , is affected by the total electron concentration in the same way as by the measured D_n . That is, $D_J \propto n_c/n_L$ becomes larger when the Fermi level is higher, so that diffusion-limited recombination becomes faster.

In DSSC, the I^-/I_3^- couple provides two electron acceptors: I_3^- and I_2^- . Recently it was shown that the recombination path depends on the illumination intensity.⁵⁹ The electron reaction with I_2^- becomes kinetically favorable only at high light

intensities. It is believed that under normal solar conditions the recombination with I_3^- dominates which makes it the only relevant process from the practical point of view.^{59,60} According to our understanding, Kopidakis et al.⁵⁶ base the characteristics of the response time on the relationship $\tau_n \propto 1/D_J$, and this leads them to select the much rarer I_2^- as the dominant acceptor, because for this low-concentration species the time for the electron to find a target for recombination would govern the τ_n .

However, the initial assumption, $\tau_n \propto 1/D_J$, is not necessary to explain the variations of τ_n . In our model, τ_{n0} is the rate constant for charge transfer, for any kind or concentration of the acceptor species. However the measured $\tau_n = (\partial n_V/\partial n_c)\tau_{n0}$ is much longer than τ_{n0} , because the Fermi level cannot decay but with equilibration of free and trapped electron density. The results of refs 32 and 33 also suggest that recombination is not governed by diffusion in configurational space but rather in energy space (energy redistribution). Here, we reached this conclusion on the assumption of the existence of a large density of traps in the bulk of particles. The results of Kopidakis et al. would also seem to support this idea of internal traps, because the intercalation of lithium into nanoparticles is affecting markedly the tailing parameter α observed in the transport parameter, D_n . However, as remarked in section 5.2, the exact effect that produces the marked departure from Boltzmann statistics is not clear yet.

In summary, the results of ref 56 do not prove the diffusion-limited recombination mechanism, that requires a scarcity of acceptor species. The experimental results can be explained more simply on the basis of the normal electron charge-transfer mechanisms in DSSC and a common origin of the Fermi-level dependence of both measured D_n and τ_n , which originates in an exponential distribution of traps in the bulk of particles. This last idea describes major features, but not so far the details, of recombination in DSSC, and it is likely that it should be improved with a more elaborated microscopic picture. In this sense, the model suggested in ref 56 is a rather interesting idea that shows the need for determining the relationship of macroscopic, steady-state time constants, to microscopic models. In particular, the connection between long-range electron transport, energy redistribution, and interfacial charge transfer requires further studies.

References and Notes

- (1) Grätzel, M. *Nature* **2001**, *414*, 338.
- (2) de Jongh, P. E.; Vanmaekelbergh, D. *Phys. Rev. Lett.* **1996**, *77*, 3427.
- (3) Cao, F.; Oskam, G.; Meyer, G. J.; Searson, P. C. *J. Phys. Chem.* **1996**, *100*, 17021.
- (4) de Jongh, P. E.; Vanmaekelbergh, D. *J. Phys. Chem. B* **1997**, *101*, 2716.
- (5) Fisher, A. C.; Peter, L. M.; Ponomarev, E. A.; Walker, A. B.; Wijayantha, K. G. U. *J. Phys. Chem. B* **2000**, *104*, 949.
- (6) Kambili, A.; Walker, A. B.; Qiu, F. L.; Fisher, A. C.; Savin, A. D.; Peter, L. M. *Physica E* **2002**, *14*, 203.
- (7) Noack, V.; Weller, H.; Eychmüller, A. *J. Phys. Chem. B* **2002**, *106*, 8514.
- (8) Kopidakis, N.; Schiff, E. A.; Park, N.-G.; van de Lagemaat, J.; Frank, A. J. *J. Phys. Chem. B* **2000**, *104*, 3930.
- (9) van de Lagemaat, J.; Frank, A. J. *J. Phys. Chem. B* **2000**, *104*, 4292.
- (10) Schlichthörl, G.; Huang, S. Y.; Sprague, J.; Frank, A. J. *J. Phys. Chem. B* **1997**, *101*, 8141.
- (11) Zaban, A.; Greenshtein, M.; Bisquert, J. *ChemPhysChem* **2003**, *4*, 859.
- (12) Bisquert, J.; Zaban, A. *Appl. Phys. A* **2003**, *77*, 507.
- (13) Nelson, J. *Phys. Rev. B* **1999**, *59*, 15374.
- (14) Willis, R. L.; Olson, C.; O'Regan, B.; Lutz, T.; Nelson, J.; Durrant, J. R. *J. Phys. Chem. B* **2002**, *106*, 7605.

- (15) Peter, L. M.; Wijayantha, K. G. U. *Electrochem. Commun.* **1999**, *1*, 576.
- (16) Abayev, I.; Zaban, A.; Fabregat-Santiago, F.; Bisquert, J. *Phys. Stat. Sol. (a)* **2003**, *196*, R4.
- (17) Schmidlin, F. W. *Philos. Mag. B* **1980**, *41*, 535.
- (18) Tiedje, T.; Rose, A. *Solid State Commun.* **1981**, *37*, 49.
- (19) Rose, A. *Concepts in Photoconductivity and Allied Problems*; Interscience: New York, 1963.
- (20) Shockley, W.; Read, W. T. J. *Phys. Rev.* **1952**, *87*, 835.
- (21) Reiss, H. *Methods of Thermodynamics*; Dover Publications: New York, 1965.
- (22) Blackmore, J. S. *Semiconductor Statistics*; Dover Publications: New York, 1962.
- (23) Bisquert, J.; Vikhrenko, V. S. *Electrochim. Acta* **2002**, *47*, 3977.
- (24) Vanmaekelbergh, D.; de Jongh, P. E. *Phys. Rev. B* **2000**, *61*, 4699.
- (25) Bisquert, J. *J. Phys. Chem. B* **2004**, *108*, 2323.
- (26) van de Lagemaat, J.; Frank, A. J. *J. Phys. Chem. B* **2001**, *105*, 11194.
- (27) Dloczik, L.; Ieperuma, O.; Lauerma, I.; Peter, L. M.; Ponomarev, E. A.; Redmond, G.; Shaw, N. J.; Uhlendorf, I. *J. Phys. Chem. B* **1997**, *101*, 10281.
- (28) Nakade, S.; Saito, Y.; Kubo, W.; Kitamura, T.; Wada, Y.; Yanagida, S. *J. Phys. Chem. B* **2003**, *107*, 8607–8611.
- (29) Bisquert, J.; Garcia-Belmonte, G.; Pitarch, A. *ChemPhysChem* **2003**, *4*, 287.
- (30) Bisquert, J. *Phys. Rev. Lett.* **2003**, *91*, 010602.
- (31) Bisquert, J.; Zaban, A.; Salvador, P. *J. Phys. Chem. B* **2002**, *106*, 8774.
- (32) Nelson, J.; Haque, S. A.; Klug, D. R.; Durrant, J. R. *Phys. Rev. B* **2001**, *63*, 205321.
- (33) Barzykin, A. V.; Tachiya, M. *J. Phys. Chem. B* **2002**, *106*, 4356.
- (34) Södergren, S.; Hagfeldt, A.; Olsson, J.; Lindquist, S. E. *J. Phys. Chem.* **1994**, *98*, 5552.
- (35) van de Lagemaat, J.; Park, N.-G.; Frank, A. J. *J. Phys. Chem. B* **2000**, *104*, 2044.
- (36) Fabregat-Santiago, F.; Garcia-Belmonte, G.; Bisquert, J.; Zaban, A.; Salvador, P. *J. Phys. Chem. B* **2002**, *106*, 334.
- (37) Fabregat-Santiago, F.; Mora-Seró, I.; Garcia-Belmonte, G.; Bisquert, J. *J. Phys. Chem. B* **2003**, *107*, 758.
- (38) Roest, A. L.; Kelly, J. J.; Vanmaekelbergh, D.; Meulenkamp, E. A. *Phys. Rev. Lett.* **2002**, *89*, 036801.
- (39) Fabregat-Santiago, F.; Garcia-Belmonte, G.; Bisquert, J.; Bogdanoff, P.; Zaban, A. *J. Electrochem. Soc.* **2003**, *150*, E293.
- (40) Zaban, A.; Meier, A.; Gregg, B. A. *J. Phys. Chem. B* **1997**, *101*, 7985.
- (41) Greene, R. F.; Callen, H. B. *Phys. Rev.* **1952**, *88*, 1387.
- (42) Oster, G.; Perelson, A.; Katchalsky, A. *Nature* **1971**, *234*, 393.
- (43) Jamnik, J.; Maier, J. *Phys. Chem. Chem. Phys.* **2001**, *3*, 1668.
- (44) Büttiker, M.; Thomas, H.; Prêtre, A. *Phys. Lett. A* **1993**, *180*, 364.
- (45) Bisquert, J. *Phys. Chem. Chem. Phys.* **2003**, *5*, 5360.
- (46) Franco, G.; Gehring, J.; Peter, L. M.; Ponomarev, E. A.; Uhlendorf, I. *J. Phys. Chem. B* **1999**, *103*, 692.
- (47) Bisquert, J. *Electrochim. Acta* **2002**, *47*, 2435.
- (48) Peter, L. M.; Duffy, N. W.; Wang, R. L.; Wijayantha, K. G. U. *J. Electroanal. Chem.* **2002**, *524–525*, 127.
- (49) Diard, J.-P.; Montella, C. *J. Electroanal. Chem.* **2003**, to be published.
- (50) Schwarzburg, K.; Willig, F. *J. Phys. Chem. B* **2003**, *107*, 3552.
- (51) Kron, G.; Egerter, T.; Werner, J. H.; Rau, W. *J. Phys. Chem. B* **2003**, *107*, 3556.
- (52) Bisquert, J. *J. Phys. Chem. B* **2002**, *106*, 325.
- (53) Bisquert, J. *J. Phys. Chem. B* **2003**, *107*, 13541.
- (54) Scher, H.; Montroll, E. W. *Phys. Rev. B* **1975**, *12*, 2455.
- (55) Nakade, S.; Saito, Y.; Kubo, W.; Kitamura, T.; Wada, Y.; Yanagida, S. *Electrochem. Commun.* **2003**, *5*, 804.
- (56) Kopidakis, N.; Benkstein, K. D.; van de Lagemaat, J.; Frank, A. J. *J. Phys. Chem. B* **2003**, *107*, 11307.
- (57) Garcia-Cañadas, J.; Fabregat-Santiago, F.; Porqueras, I.; Person, C.; Bisquert, J.; Garcia-Belmonte, G. *Solid State Ionics*, submitted.
- (58) van de Krol, R.; Goossens, A.; Schoonman, J. *J. Phys. Chem. B* **1999**, *103*, 7151.
- (59) Bauer, C.; Boschloo, G.; Mukhtar, E.; Hagfeldt, A. *J. Phys. Chem. B* **2002**, *106*, 12693.
- (60) Montanari, I.; Nelson, J.; Durrant, J. R. *J. Phys. Chem. B* **2002**, *106*, 12203.